

Probing the Structural Requirements of Peptoids That Inhibit HDM2–p53 Interactions

Toshiaki Hara,[†] Stewart R. Durell,[†] Michael C. Myers,[‡] and Daniel H. Appella^{*,§}

Contribution from the Laboratory of Cell Biology, NCI, National Institutes of Health, DHHS, Bethesda, Maryland 20892, Department of Chemistry, Northwestern University, Evanston, Illinois 60208, and Laboratory of Bioorganic Chemistry, NIDDK, National Institutes of Health, DHHS, Bethesda, Maryland 20892

Received September 14, 2005; E-mail: appellad@nidk.nih.gov

Abstract: Many cellular processes are controlled by protein–protein interactions, and selective inhibition of these interactions could lead to the development of new therapies for several diseases. In the area of cancer, overexpression of the protein, human double minute 2 (HDM2), which binds to and inactivates the protein p53, has been linked to tumor aggressiveness and drug resistance. In general, inhibition of protein–protein interactions with synthetic molecules is challenging and currently remains a largely uncharted area for drug development. One strategy to create inhibitors of protein–protein interactions is to recreate the three-dimensional arrangement of side chains that are involved in the binding of one protein to another, using a nonnatural scaffold as the attachment point for the side chains. In this study, we used oligomeric peptoids as the scaffold to begin to develop a general strategy in which we could rationally design synthetic molecules that can be optimized for inhibition of protein–protein interactions. Structural information on the HDM2–p53 complex was used to design our first class of peptoid inhibitors, and we provide here, in detail, the strategy to modify peptoids with the appropriate side chains that are effective inhibitors of HDM2–p53 binding. While we initially tried to develop rigid, helical peptoids as HDM2 binders, the best inhibitors were surprisingly peptoids that lacked any helix-promoting groups. These results indicate that starting with rigid peptoid scaffolds may not always be optimal to develop new inhibitors.

Introduction

Over the last 20 years, many connections between cancer and the protein p53 have been established. In normal cells, p53 can be inactivated due to association with the protein human double minute 2 (HDM2). When p53 is inactive, cells are able to grow and proliferate. Under conditions of cellular stress or genomic damage, p53 activity is turned on. Once activated, p53 functions as a transcription factor to promote production of other proteins that result in cell cycle arrest or apoptosis. In the majority of cancers, the mechanism of action of p53 is defective. In one-half of all cancers, p53 acquires a genetic mutation that prevents DNA binding and therefore inhibits p53 from acting as a transcription factor. In a large number of other cancers, wild-type p53 protein is present, but the cancer cells overexpress negative regulators of p53, such as HDM2. Overexpression of HDM2 has been linked to tumor aggressiveness and drug resistance, and inhibition of HDM2 can restore p53 function and prevent cancer growth.^{1,2}

The structural detail of HDM2 was first revealed in 1996 by a crystal structure of the complex formed between HDM2 and a peptide derived from the transactivation domain of p53

(residues 15–29),³ which greatly stimulated the search for HDM2 inhibitors with chemotherapeutic activity.^{4–6} In the crystal, the N-terminal domain of HDM2 (residues 17–125) binds a conserved fragment of the N-terminal, transactivation domain of p53. The HDM2 fragment has two structurally similar subdomains arranged to form a large, nonpolar cleft that binds the p53 fragment. The latter forms an amphipathic α -helix between residues 18–26, while both ends are in extended conformations. As seen in Figure 1, the tandem F19, W23, and L26 residues of p53 pack tightly and deeply in the nonpolar crevice of HDM2. Within this complex, there are no salt-bridges, and only two intermolecular hydrogen bonds. The stability of the complex is primarily due to the hydrophobic interactions involving the three cleft-binding residues, as confirmed by amino acid substitution studies.⁷

Considerable effort has been expended to exploit HDM2 as a molecular target to kill cancer cells, leading to greater understanding of the variety of pathways and mechanisms in which it is involved (both dependent and independent of p53).⁶ Inhibition of HDM2 binding to p53 has recently emerged as a

[†] Laboratory of Cell Biology, NIH.

[‡] Northwestern University.

[§] Laboratory of Bioorganic Chemistry, NIH.

(1) Momand, J.; Wu, H. H.; Dasgupta, G. *Gene* **2000**, *242*, 15–29.

(2) Chène, P. *Nat. Rev. Cancer* **2003**, *3*, 102–109.

(3) Kussie, P. H.; Gorina, S.; Marechal, V.; Elenbaas, B.; Moreau, J.; Levine, A. J.; Pavletich, N. P. *Science* **1996**, *274*, 948–953.

(4) Shair, M. D. *Chem. Biol.* **1997**, *4*, 791–794.

(5) Chène, P. *Mol. Cancer Res.* **2004**, *2*, 20–28.

(6) Buolamwini, J. K.; Addo, J.; Kamath, S.; Patil, S.; Mason, D.; Ores, M. *Curr. Cancer Drug Targets* **2005**, *5*, 57–68.

(7) Böttger, A.; Böttger, V.; Garcia-Echeverria, C.; Chene, P.; Hochkeppel, H. K.; Sampson, W.; Ang, K.; Howard, S. F.; Picklesley, S. M.; Lane, D. P. *J. Mol. Biol.* **1997**, *269*, 744–756.

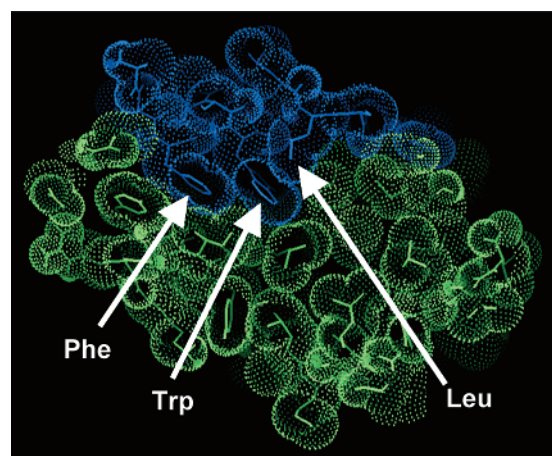


Figure 1. Cross-sectional slice of the crystal structure of the p53 peptide (blue) bound to HDM2 (green). Arrows highlight the three hydrophobic residues on the p53 peptide that are critical for binding.

common strategy to restore wild-type p53 activity.⁴ In this context, a variety of effective HDM2 inhibitors have been independently identified either from natural products or using structure-based drug design and/or combinatorial screening.^{5,8–10} The best inhibitors of HDM2–p53 binding are either small molecules that are very hydrophobic or oligomeric molecules that arrange hydrophobic side chains into the same three-dimensional arrangement as the bound p53 helix. While a number of these have been demonstrated to normalize levels of p53 and kill cancer cells in culture, relatively few have demonstrated biological activity in animal studies, and none has been employed in clinical trials. Therefore, the development of additional HDM2 inhibitors is still necessary.

In this paper, we describe our development of a competitive binding inhibitor based on oligomeric peptoids. The peptoid monomer (or N-substituted glycine) is similar to a regular amino acid, except that the side chain is attached to the backbone nitrogen atom instead of the α -carbon.¹¹ Peptoids are a particularly attractive choice for making peptide-like compounds because a wide variety of side chains can be attached to the peptoid backbone and peptoids are resistant to proteolytic digestion. For these reasons, peptoids have been studied as potential agonists and antagonists in a number of biological

systems, including “high-affinity” tri-peptoid ligands for two 7-transmembrane G-protein-coupled receptor proteins, peptide–peptoid hybrid ligands for Src homology 3 (SH3) protein domains, and tri-peptoid blockers of the Vanilloid receptor subunit 1 (VR1) and *N*-methyl-D-aspartate (NMDA) receptor channels associated with pain and neurodegeneration.¹²

Another important feature of peptoids is that the backbone can be sterically biased to form a helical conformation by incorporating chiral side chains into the oligomer.¹³ A rigid helical scaffold can predetermine the docked conformation to a protein, thus providing more favorable entropy for binding. This has been exploited to form amphipathic peptoid helices to mimic the antibacterial Magainin peptide and the lung surfactant Protein C for extracellular medicinal applications.¹⁴ Recently, X-ray crystal structure studies have confirmed that the helical structure is preserved for a wide variety of side chain sizes, including both aromatic and aliphatic classes.¹⁵ The chiral-peptoid helix is similar to a type-I polyproline helix, in which the amide bonds are *cis*, and the carbonyl groups point with the oxygens toward the N-terminus, causing the electrostatic dipole moment to be the reverse of standard α -helices. Because the helical conformation is dictated by steric constraints, and not hydrogen bonds, as with a regular protein, it is able to persist in both aqueous and nonpolar solvents and under a broad range of pH and temperature conditions.^{11,16} Helical polypeptides have well-characterized circular dichroism (CD) spectra, similar to a regular protein α -helix, which provides a rapid probe of the conformational state. In addition, at least some peptoids are pharmacologically biocompatible and are currently being examined for a variety of therapeutic purposes.¹⁷

In this study, we reveal several important molecular features of HMD2-binding peptoids that are required to achieve binding to HDM2. Most of the initial peptoid designs were guided by molecular modeling of a helical peptoid bound to HDM2; however, substantial experimentation with new peptoid side chains was essential to obtain HDM2 binding. Direct experimental comparisons of the binding affinity of our peptoid inhibitors with that of the p53 peptide, as well as the recently developed small molecule antagonist Nutlin-3¹⁸ and another HDM2-binding peptoid⁹ isolated from a combinatorial screen, are also presented. While we approached the design of peptoid inhibitors starting from a stable helix that contained chiral side chains at every position, to increase aqueous solubility we had to incorporate achiral side chains with polar functional groups. Unfortunately, chiral versions of these side chains are not easily synthesized. Therefore, as more achiral side chains were incorporated in the peptoids to promote aqueous solubility, helical stability was diminished. In this study, our results

- (8) Klein, C.; Vassilev, L. T. *Br. J. Cancer* **2004**, *91*, 1415–1419.
 (9) Alluri, P. G.; Reddy, M. M.; Bachhawat-Sikder, K.; Olivios, H. J.; Kodadek, T. *J. Am. Chem. Soc.* **2003**, *125*, 13995–14004.
 (10) (a) Duncan, S. J.; Gruschow, S.; Williams, D. H.; McNicholas, C.; Purewal, R.; Hajek, M.; Gerlitz, M.; Martin, S.; Wrigley, S. K.; Moore, M. *J. Am. Chem. Soc.* **2001**, *123*, 554–560. (b) Kumar, S. K.; Hager, E.; Pettit, C.; Gurulingappa, H.; Davidson, N. E.; Khan, S. R. *J. Med. Chem.* **2003**, *46*, 2813–2815. (c) Galatin, P. S.; Abraham, D. J. *J. Med. Chem.* **2004**, *47*, 4163–4165. (d) Sakurai, K.; Chung, H. S.; Kahne, D. *J. Am. Chem. Soc.* **2004**, *126*, 16288–16289. (e) Kritzer, J. A.; Lear, J. D.; Hodsdon, M. E.; Schepartz, A. *J. Am. Chem. Soc.* **2004**, *126*, 9468–9469. (f) Fasan, R.; Dias, R. L. A.; Moehle, K.; Zerbe, O.; Vrijbloed, J. W.; Obrecht, D.; Robinson, J. A. *Angew. Chem., Int. Ed.* **2004**, *43*, 2109–2112. (g) Zhong, H.; Carlson, H. A. *Proteins* **2004**, *58*, 222–234. (h) Grasberger, B. L.; et al. *J. Med. Chem.* **2005**, *48*, 909–912. (i) Yin, H.; Lee, G. I.; Park, H. S.; Payne, G. A.; Rodriguez, J. M.; Sehti, S. M.; Hamilton, A. D. *Angew. Chem., Int. Ed.* **2005**, *44*, 2704–2707. (j) Ding, K.; et al. *J. Am. Chem. Soc.* **2005**, *127*, 10130–10131. (k) Murray, J. K.; Farooqi, B.; Sadowsky, J. D.; Scalf, M.; Freund, W. A.; Smith, L. A.; Chen, J.; Gellman, S. H. *J. Am. Chem. Soc.* **2005**, *127*, 13271–13280. (l) Kritzer, J. A.; Leudtke, N. W.; Harker, E. A.; Schepartz, A. *J. Am. Chem. Soc.* **2005**, *127*, 14584–14585. (m) Tsukamoto, S.; Yoshida, T.; Hosono, H.; Ohta, T.; Yokosawa, H. *Bioorg. Med. Chem. Lett.* **2005**, *16*, 69–71.
 (11) (a) Kirshenbaum, K.; Barron, A. E.; Goldsmith, R. A.; Armand, P.; Bradley, E. K.; Truong, K. T.; Dill, K. A.; Cohen, F. E.; Zuckermann, R. N. *Proc. Natl. Acad. Sci. U.S.A.* **1998**, *95*, 4303–4308. (b) Kirshenbaum, K.; Zuckermann, R. N.; Dill, K. A. *Curr. Opin. Struct. Biol.* **1999**, *9*, 530–535.

- (12) (a) Zuckermann, R. N.; et al. *J. Med. Chem.* **1994**, *37*, 2678–2685. (b) Nguyen, J. T.; Porter, M.; Amoui, M.; Miller, W. T.; Zuckermann, R. N.; Lim, W. A. *Chem. Biol.* **2000**, *7*, 463–473. (c) Planells-Cases, R.; et al. *J. Pharmacol. Exp. Ther.* **2002**, *302*, 163–173. (d) Garcia-Martinez, C.; et al. *Proc. Natl. Acad. Sci. U.S.A.* **2002**, *99*, 2374–2379.
 (13) Armand, P.; Kirshenbaum, K.; Falicov, A.; Dunbrack, R. L., Jr.; Dill, K. A.; Zuckermann, R. N.; Cohen, F. E. *Fold Des.* **1997**, *2*, 369–375.
 (14) (a) Patch, J. A.; Barron, A. E. *J. Am. Chem. Soc.* **2003**, *125*, 12092–12093. (b) Wu, C. W.; Seurnyck, S. L.; Lee, K. Y.; Barron, A. E. *Chem. Biol.* **2003**, *10*, 1057–1063.
 (15) Wu, C. W.; Kirshenbaum, K.; Sanborn, T. J.; Patch, J. A.; Huang, K.; Dill, K. A.; Zuckermann, R. N.; Barron, A. E. *J. Am. Chem. Soc.* **2003**, *125*, 13525–13530.
 (16) Sanborn, T. J.; Wu, C. W.; Zuckermann, R. N.; Barron, A. E. *Biopolymers* **2002**, *63*, 12–20.
 (17) Gibbons, J. A.; et al. *J. Pharmacol. Exp. Ther.* **1996**, *277*, 885–899.
 (18) Vassilev, L. T.; et al. *Science* **2004**, *303*, 844–848.

surprisingly demonstrate that fewer chiral side chains in the peptoid result in better HDM2 binding.

Experimental Section

1. Molecular Modeling. Atomic coordinates for all of the models were generated and energy minimized with the CHARMM molecular mechanics computer program,^{19a} combined with the CHARMM22 versions of the all-atom topology and parameter sets^{19b} to describe the residues. Whereas the HDM2 model could be formed by the common amino acid residues already present in the package, the topologies for the different peptoids were “manually” created. This was accomplished by taking side chain topology fragments from the default set of common residues and grafting them onto the amide nitrogen of glycine. Additional customizations were made to create the stereogenic centers and/or alter other aspects of the side chains. It should be emphasized that no attempt was made to use the potential energy functions to make de novo predictions of the conformation of the peptoid beyond the obvious covalent geometry, or the binding affinity of the real peptoid to HDM2 in solution.

The primary design goal was to create a helical polypeptoid with phenylalanine, tryptophan, and leucine side chains along one side to reproduce as closely as possible the relative orientations of the F19, W23, and L26 residues of the bound p53 peptide, which are the most important for binding.^{7,20} To start, the backbone of the polypeptoid was manipulated into the ideal helical conformation described by Armand and co-workers¹³ using molecular graphics software. We always chose to use right-handed helices, which are formed from the *S* enantiomers of chiral peptoid monomers. The model was then docked to HDM2 by overlaying the cleft-binding residues of p53 in the crystal structure. Energy minimization was then used to remove atomic overlaps and optimize any available hydrogen bonds and/or salt-bridges.

As described in the Results, the procedure was iteratively repeated with additional modifications to the peptoid model to enhance the overlap of the cleft-binding residues and increase the solubility and binding affinity. It should be emphasized that no attempt was made to use the calculated binding energies of the models as a predictor of the binding affinity of the real polypeptoid to HDM2 in solution. Unfortunately, the current state of potential energy functions and achievable time-scales of dynamic simulations are insufficient to accurately sample the conformational space and calculate the relevant thermodynamic factors (especially of the hydrophobic effect). Rather, the three-dimensional computer models served to examine the steric goodness-of-fit of the peptoid to HDM2 and to devise chemical improvements for the subsequent rounds of synthesis and testing.

2. Peptoid Synthesis. All peptoids were synthesized using the submonomer approach,²¹ using commercially available amines or synthetically prepared ones. In some cases, new amines were made that had not previously been incorporated into peptoids. These were specifically made to adjust the properties of the peptoids to promote interactions with HDM2 or to enhance aqueous solubility. The new amines incorporated into peptoids are shown in Figure 2, and the details of the synthetic work are described in the Supporting Information.

3. Binding Assays. The protein HDM2 was expressed following published procedures,³ which are summarized in the Supporting Information. To determine the ability of each peptoid to inhibit p53–HDM2 association, a reported fluorescence polarization competition assay with a fluorescein-labeled p53 peptide composed of residues 15–

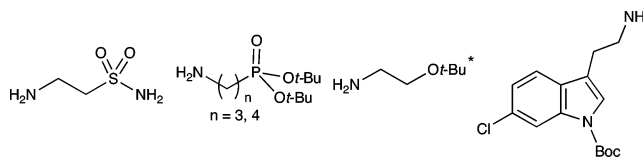


Figure 2. Synthetically prepared amines that were incorporated into peptoids to promote interactions with HDM2 or promote aqueous solubility. (*Ethanolamine has been previously incorporated into peptoids,⁹ but in this work we introduced a *t*-Bu ether protecting group.)

29 (which will be abbreviated as Flu–p53(15–29)) was used.²² The degrees of displacement of the labeled peptide from HDM2 at a series of concentrations of added peptoid were measured, and then the IC₅₀ values for inhibition were calculated by regression analysis. Isothermal titration calorimetry was performed according to previously published procedures,²³ and experimental details are provided in the Supporting Information. Nutlin compounds were generous gifts from Dr. L. T. Vassilev and Hoffman-LaRoche, Inc., Nutley, NJ.

Results

1. Initial Peptoid Design. To reproduce the relative positioning of the F19, W23, and L26 residues of the bound p53 fragment, it was necessary to account for the structural differences between the ideal type-1 polyproline helix of the peptoid and the standard α -helix of regular peptides. One difference is that the peptoid helix is more tightly wound than that of the peptide, with only 3.0 residues per turn as compared to 3.6. Thus, simply transposing the peptide sequence to the peptoid results in a helix in which the alignment of these three residues is lost. Fortunately, this could be corrected by deleting one position between the phenylalanine and tryptophan residues in the peptoid sequence, thus going from (*i*, *i*+4) to (*i*, *i*+3). Because the tryptophan and leucine are already one position closer in the p53 sequence, the misalignment in the peptoid helix conformation is less. In addition, this part of the bound p53 helix is already in a distorted, less tightly wound conformation. Thus, it was not necessary to alter the spacing between these two residues in the peptoid sequence. The other relevant structural difference between the two helices is that the side chains project out at different angles. This has a critical effect on how they orient and fit in the contours of the hydrophobic cleft of HDM2. Fortunately, this problem could be overcome by adding an extra methylene group to both the phenylalanine and the tryptophan peptoid side chains, which allows for greater orientational variation of the phenyl and indole rings.

As shown in Figure 3, these modifications allow for a relatively close structural reproduction of the main p53 binding residues. Modeling of the complex demonstrates that only the phenyl and indole rings need to fit into tightly contoured wells. In contrast, the region of the HDM2 cleft to which the leucine binds is relatively shallow and extended, and thus able to accommodate a repositioning of this third hydrophobic residue. This is consistent with the peptide mutagenesis results of Böttger and co-workers,⁷ in which the phenylalanine and tryptophan were essential for activity, but the leucine could be changed to isoleucine, methionine, or valine and still maintain partial activity.

2. Initial Peptoids – Synthesis, Secondary Structure, Aqueous Solubility, and Binding. The first step was to build

(19) (a) Brooks, B. R.; Brucoleri, R. E.; Olafson, B. D.; States, D. J.; Swaminathan, S.; Karplus, M. *J. Comput. Chem.* **1983**, *4*, 187–217. (b) MacKerell, A. D.; et al. *J. Phys. Chem. B* **1998**, *102*, 3586–3616.
(20) García-Echeverría, C.; Chène, P.; Blommers, M. J.; Furet, P. *J. Med. Chem.* **2000**, *43*, 3205–3208.
(21) Figliozzi, G. M.; Goldsmith, R.; Ng, S. C.; Banville, S. C.; Zuckermann, R. N. *Methods Enzymol.* **1996**, *267*, 437–447.

(22) (a) Knight, S. M. G.; Umezawa, N.; Lee, H.-S.; Gellman, S. H.; Kay, B. K. *Anal. Biochem.* **2002**, *300*, 230–236. (b) Zhang, R.; Mayhood, T.; Lipari, P.; Wang, Y.; Durkin, J.; Syto, R.; Gesell, J.; McNemar, C.; Windsor, W. *Anal. Biochem.* **2004**, *331*, 138–146.
(23) Houtman, J. C. D.; et al. *Biochemistry* **2004**, *43*, 4170–4178.

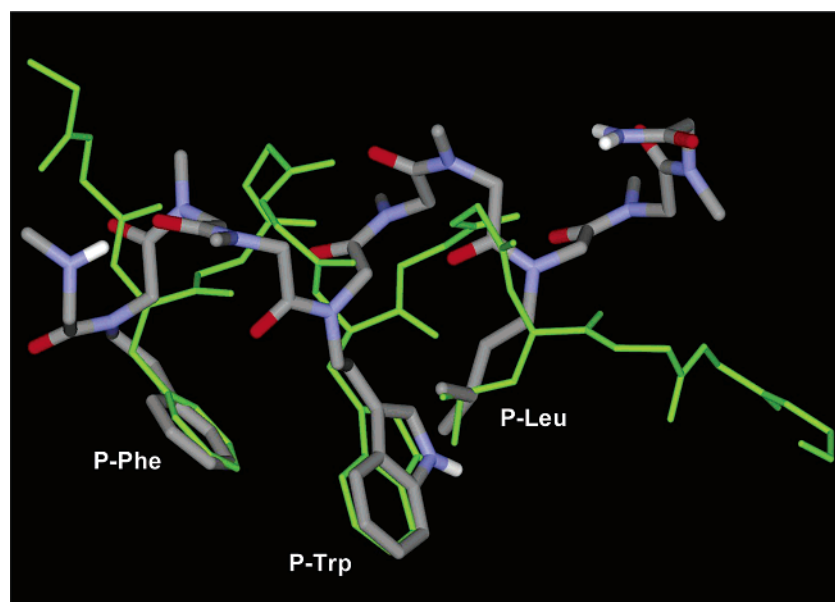


Figure 3. Structural comparison of the three hydrophobic cleft-binding residues of the bound p53 peptide (green structure) and the designed peptoid helix (based on peptoid PS2 in the Supporting Information). The peptoid helix shown is the result of energy minimization while docked in the binding cleft of HDM2. Peptoid side chains are designated with a P followed by the amino acid side chain that they mimic. (Additional side chains of the peptoid and peptide are omitted for clarity.)

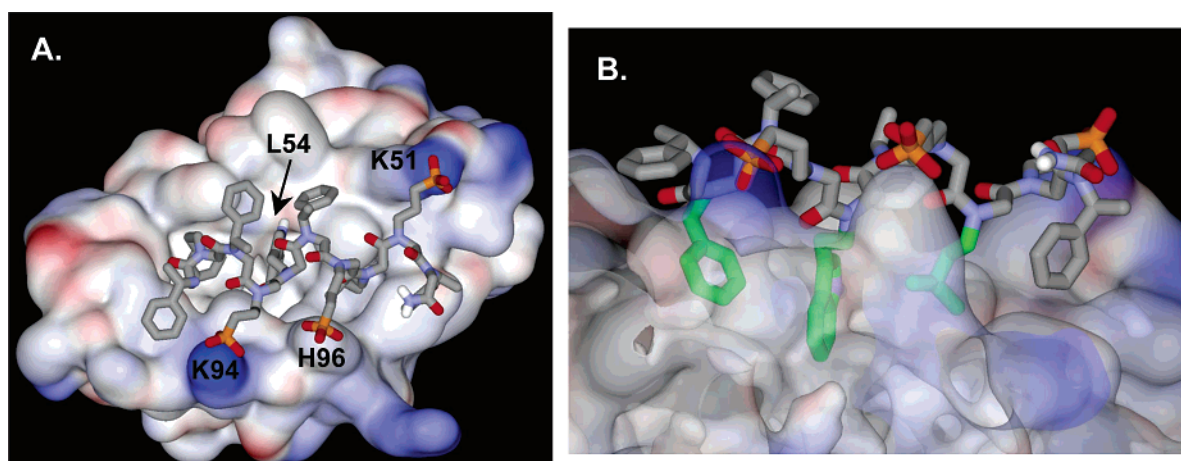


Figure 4. (A) Model of peptoid 2 docked to HDM2. The surface of HDM2 is shown as an electrostatic potential energy map. HDM2 amino acids with which the peptoid side chains could interact are labeled. (B) Side view showing hydrophobic peptoid side chains (green) bound in the HDM2 crevice. HDM2 is shown as a transparent surface.

a plain, helical peptoid from 10 chiral (*S*)-*N*-(1-phenylethyl)-glycine subunits (peptoid PS1, Supporting Information) to serve as a reference point for the CD spectrum of a helical peptoid. In acetonitrile, peptoid PS1 has a far-UV CD spectrum typical of a peptoid in a right-handed helical conformation, with two minima at 219 and 205 nm, and a maximum at 193 nm (Figure S3, Supporting Information). Our first attempt to make an HDM2-binding peptoid centered on introducing achiral phenylalanine, tryptophan, and leucine peptoid analogue subunits at positions 3, 6, and 9 of peptoid PS1, as is called for in the original design (see peptoid PS2, Supporting Information). In acetonitrile, the CD spectrum of peptoid PS2 retains the characteristic structure of a helix, but with the magnitude of molar ellipticity reduced approximately 30% as compared to peptoid PS1 (Figure S3, Supporting Information). This likely reflects the reduction in the number of chiral subunits in the peptoid decamer and indicates a less stable helical conformation in solution. Data on the binding of peptoid PS2 to HDM2 could not be obtained

due to the poor aqueous solubility of this peptoid. To make a more water-soluble analogue, three achiral peptoid glutamic acid residues were substituted into the sequence to create peptoid 1 (Figure 5). Still assuming a helical conformation for the bound inhibitor, these new side chains were designed to form salt-bridges with the K94, H96, and K51 residues of HDM2 at the edges of the binding cleft (modeling not shown). In an effort to keep at least one chiral subunit at the C-terminus, the phenylalanine, tryptophan, and leucine analogues were shifted to positions 2, 5, and 8, and the glutamic acid analogues were put at positions 4, 7, and 9. Peptoid 1 was found to be partially soluble in water (pH 7.2, 10 mM Tris HCl, 10 mM NaCl, 0.5 mM EDTA), but was inactive in the fluorescence polarization binding assay (results not shown). With the number of chiral subunits reduced to only 4 out of 10, the CD spectrum of peptoid 1 indicated a further destabilization of the helical conformation in aqueous solution, especially by the large diminution of the molar ellipticity of the positive peak at 193 nm (Figure 6).

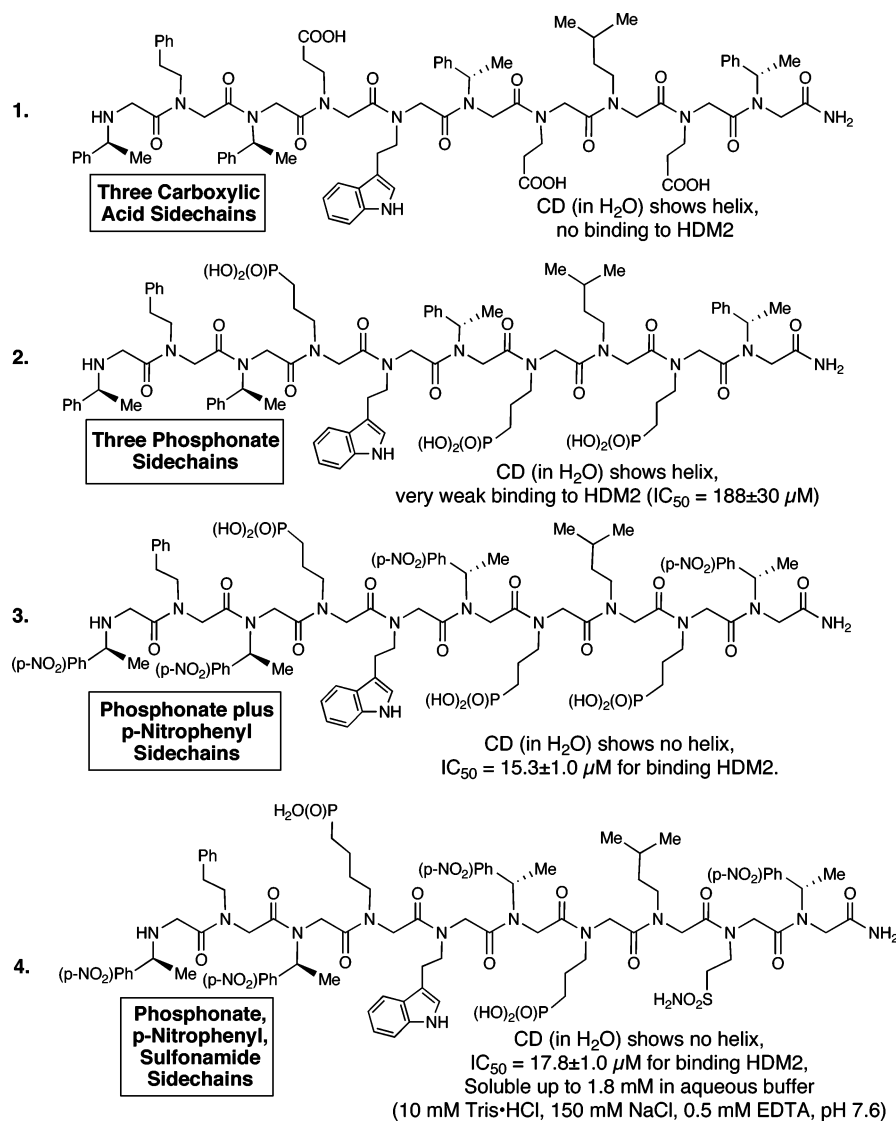


Figure 5. Initial peptoids synthesized to test for HDM2 binding, helicity, and water solubility.

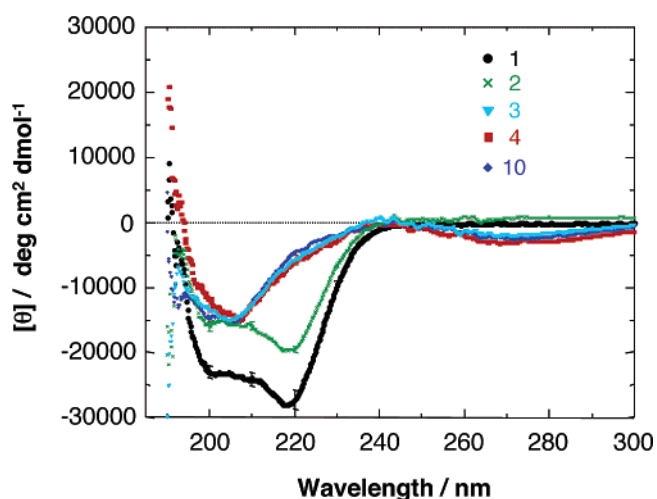


Figure 6. CD spectra of peptoids 1–4 and 10. The spectra were measured in Tris buffer (10 mM Tris, 10 mM NaCl, 0.5 mM EDTA, pH 7.6) at room temperature. Peptoid concentration was 60 μM for all samples.

Interestingly, the two negative peaks at 219 and 205 nm were approximately the same as for peptide PS2.

To further increase the aqueous solubility, peptoid 2 was synthesized with three phosphonates replacing the carboxylates.

Synthesis of the phosphonate-containing peptoid monomer relied on the development of two new building block amines (see Supporting Information for synthesis). As predicted, peptoid 2 was more soluble in water using the same buffer conditions as for peptoid 1, but a slightly more basic pH of 7.6 was optimal for solubility. However, the new side chains resulted in a further destabilization of the helical conformation in solution, as indicated by further reduction in the magnitude of the two negative peaks and complete elimination of the positive peak in the CD spectrum as compared to peptoid PS1 (Figure 6). Fortunately, peptoid 2 was the first to demonstrate at least weak (IC₅₀ = 188 μM) competitive binding to HDM2 (Figure 11A and Table 1). This binding may be due to the greater electrostatic attraction of the phosphonates to the positively charged lysine residues around the cleft of HDM2, as indicated by the modeling of peptoid 2 bound to HDM2 presented in Figure 4. In this model, the phosphonate side chains of the peptoid interact favorably with two lysines and one histidine on the surface of the protein, while the indole side chain of the peptoid forms a hydrogen bond to the carbonyl oxygen of leucine 54.

In an effort to increase the hydrophilicity of the phenylethyl side chains, peptoid 3 was synthesized with *para*-nitro groups

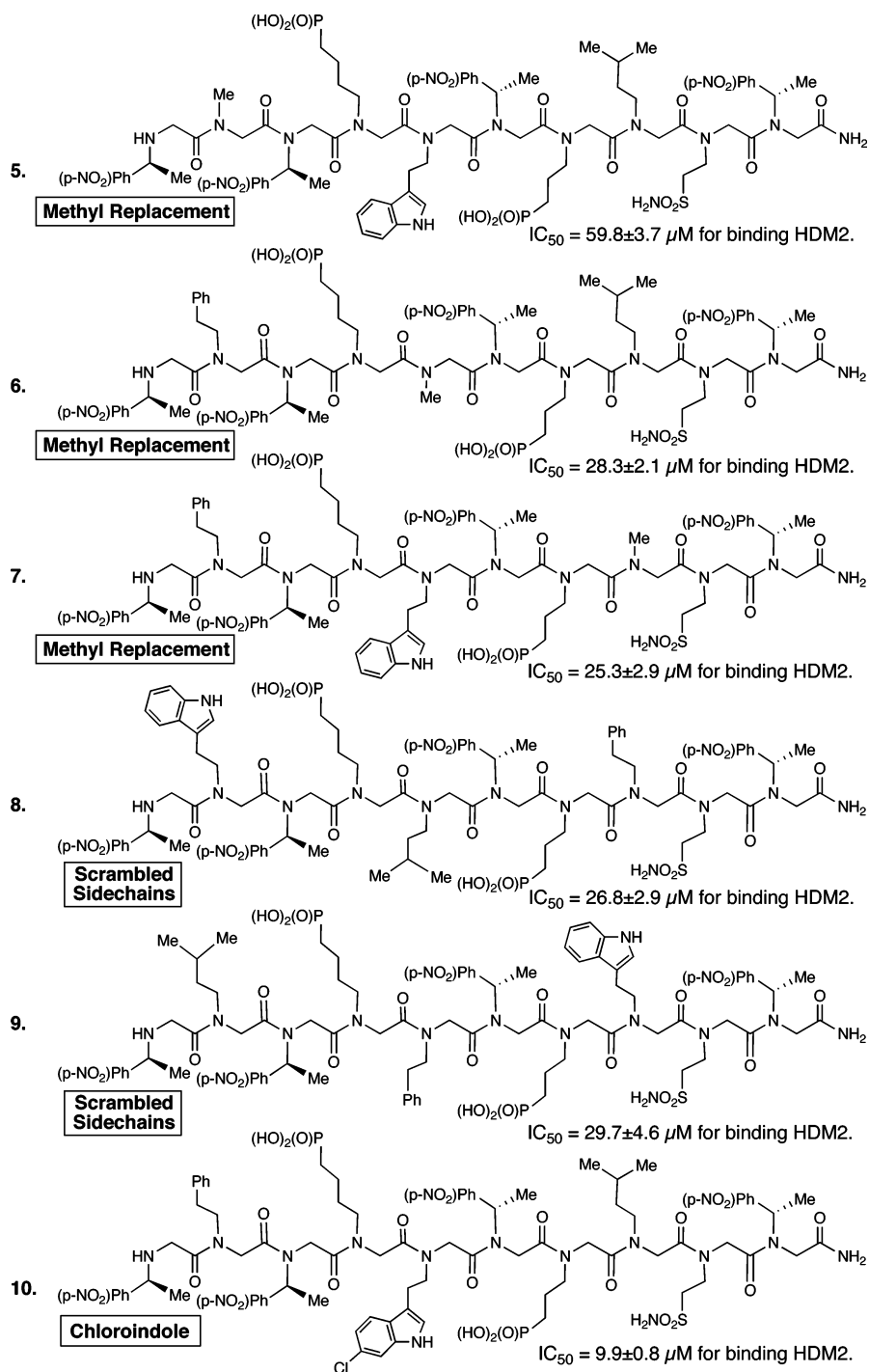


Figure 7. Peptoids synthesized to probe the importance of hydrophobic interactions (numbering continues from Figure 5).

on the phenyl rings, that is, using (*S*)-*N*-(*p*-nitrophenylethyl)-glycine peptoid subunits. This analogue has been previously examined and found to promote the same helical conformation as the nonsubstituted peptoids.¹¹ Interestingly, the CD spectrum of peptoid 3 in solution was found to significantly differ from that of peptoid 2, with total abolition of the negative peak at 219 nm (Figure 6). Rather, the spectrum resembles that of an acetylated monomer of (*S*)-*N*-(*p*-nitrophenylethyl)glycine in acetonitrile shown in Figure 4 of the paper published by Kirshenbaum and co-workers,^{11a} which also has a single negative peak at approximately 205 nm and a molar ellipticity of approximately 17×10^{-3} deg cm²/dmol. Because the monomer is not physically able to form a helix, this suggests

that peptoid 3 is not in a helical conformation in aqueous solution. Fortunately, however, peptoid 3 showed a significant increase in the binding affinity to HDM2, with an IC_{50} of 15 μM (Figure 11A and Table 1), only 5 times larger than that of the p53 peptide. While the exact reasons for the improvements in binding are unclear, it is possible that the nitro groups promote alternative conformations of the peptoid that are more complementary to the HDM2 binding site and/or that favorable hydrogen bonds between the nitro groups and proximal residues on HDM2 are formed. With the improvements in binding seen with peptoid 3, we pursued this structure as a lead compound and made additional modifications to reveal the essential features and enhance the binding affinity.

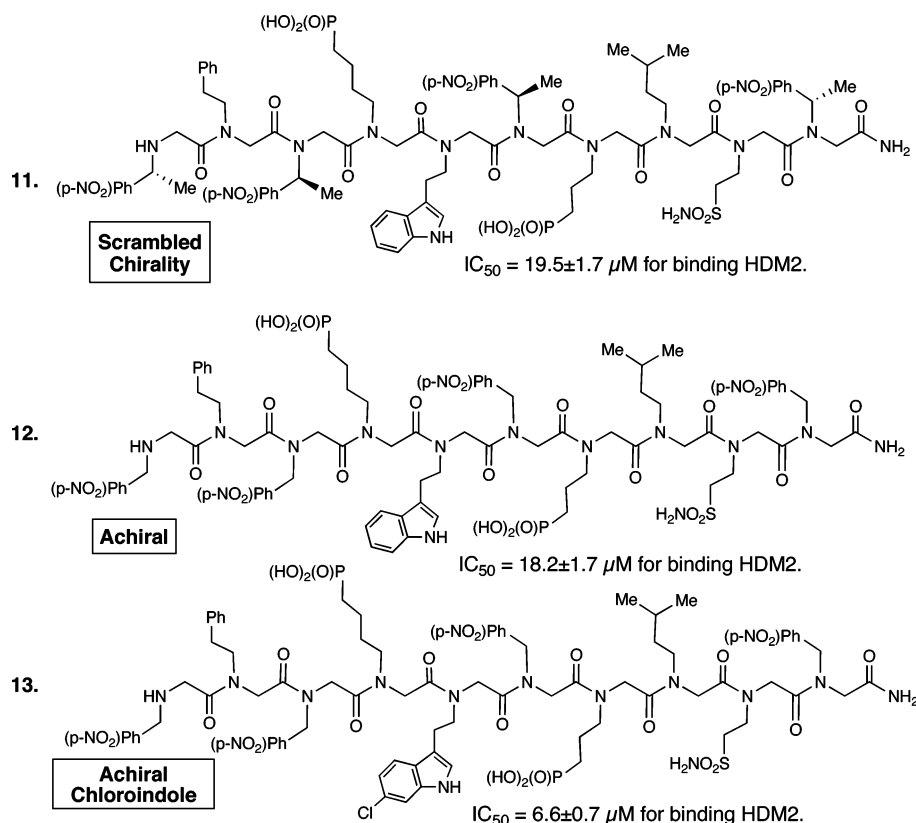


Figure 8. Effects of peptoid chirality on HDM2 binding (numbering continues from Figure 7).

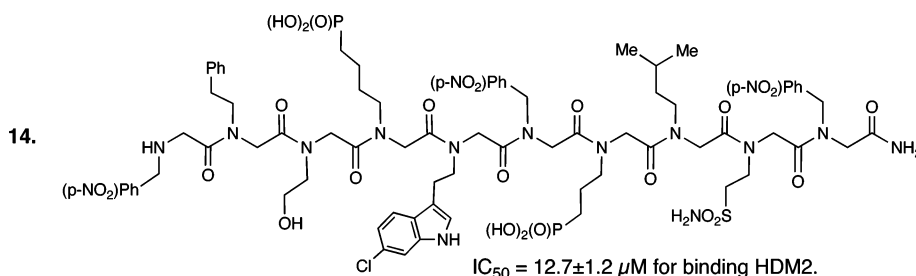


Figure 9. Effect of replacing a *p*-nitrophenyl group on HDM2 binding.

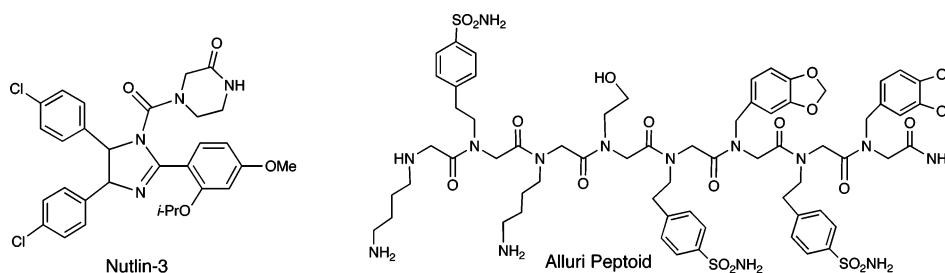


Figure 10. Structures of Nutlin-3 and the Alluri peptoid used to compare binding to HDM2.

3. Charged Peptoid Residues. To attain biological activity, it will ultimately be necessary for the peptoid to cross cell membranes. To facilitate this, we sought to reduce the number of phosphonate groups so that there was a minimum of anionic charge. Therefore, peptoids were made in which the phosphonate side chains were selectively replaced with sulfonamides (see peptoid 4 in Figure 5 and peptoids PS3 and PS4 in Figure S1 of the Supporting Information). Although sulfonamides are neutral in overall charge, the two oxygens on the sulfur have partial negative charges that may still interact with the proximal positively charged residues of HDM2. Peptoid 4, with one

sulfonamide substitution at position 9, retained good water solubility, and the binding affinity to HDM2 was largely unaffected as compared to peptoid 3 (Figure 11A and Table 1). In addition, the CD spectrum was very similar (Figure 6). However, additional sulfonamide substitutions at positions 4 and 7 resulted in peptoids that were insoluble in aqueous solutions. Therefore, the sequence of two phosphonates and one sulfonamide, as in peptoid 4, was incorporated in the development of subsequent peptoids.

4. Peptoid Length. The next series of peptoids were designed to probe the effect of oligomer length on HDM2 binding.

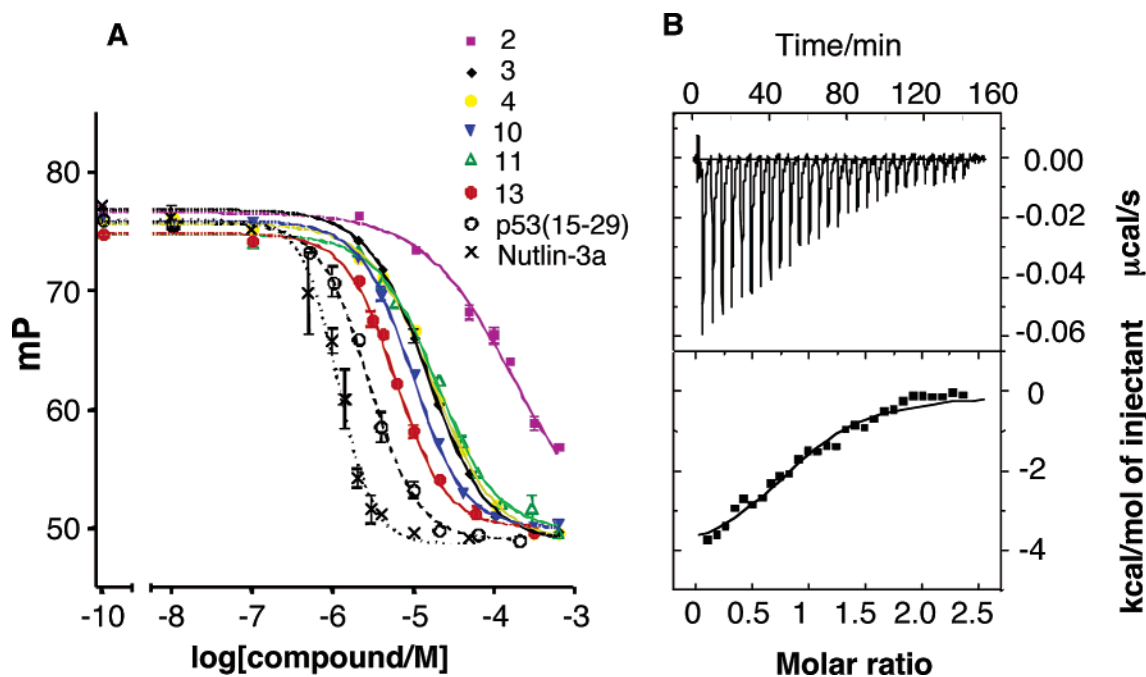


Figure 11. Binding and inhibitory activity of peptides, p53 peptide, and Nutlin-3. (A) Fluorescence polarization assay: Displacement of HDM2 bound Flu-p53(15–29) by peptides and reported competitors. Compounds were titrated to preincubated HDM2 (2.2 μM)–Flu-p53(15–29) (30 nM). (B) ITC assay: Binding isotherm for the interaction of HDM2 with peptide 13. The titration involved the injection of 7.5 μL of the peptide solution (125 μM) into HDM2 (8.5 μM). All experiments were performed at 25 $^{\circ}\text{C}$ in Tris buffer (10 mM Tris HCl, 150 mM NaCl, 1 mM β -mercaptoethanol, 0.5 mM EDTA, pH 7.6), and the data were analyzed as described in the Supporting Information.

Table 1. IC_{50} Values Obtained from Fluorescence Polarization

entry	IC_{50} (μM) ^a	entry	IC_{50} (μM) ^a
peptoid		peptoid	1
1	NB ^b	10	99 ± 0.8
2	188 ± 30	11	19.5 ± 1.7
3	15.3 ± 1.0	12	18.2 ± 1.7
4	17.8 ± 1.0	13	6.6 ± 0.7
5	59.8 ± 3.7	14	12.7 ± 1.2
6	28.3 ± 2.1	Alluri	NB ^b
7	25.3 ± 2.9	Nutlin	
8	26.8 ± 2.9	3a	1.2 ± 0.3
9	29.7 ± 4.6	3b	17.7 ± 3.3

^a Concentration necessary to displace 50% of HDM2-bound Flu-p53(15–29). For comparison, the p53(15–29) peptide was bound with an $\text{IC}_{50} = 3.0 \pm 0.3$ μM . ^b NB = no detectable binding.

Adding an extra (*S*)-*N*-(*p*-nitrophenylethyl)glycine residue to the N- and C-termini of peptoid 4 does not have a significant impact on the binding affinity to HDM2 (peptoids PS5, PS6, and Table S1 in the Supporting Information). However, the binding affinity was significantly reduced with a shorter peptoid that lacked the N- and C-terminal (*S*)-*N*-(*p*-nitrophenylethyl)glycines of peptoid 4 (peptoid PS7). In this case, the IC_{50} increased to 222 μM , similar to that of peptoid 2. Therefore, the peptoid length was maintained at 10 residues for subsequent development, with the chiral (*S*)-*N*-(*p*-nitrophenylethyl)glycine residues maintained at the N- and C-termini.

5. Cleft-Binding Residues. To test the assumption that the hydrophobic phenylalanine, tryptophan, and leucine side chain mimics of peptoid 4 each bind in the nonpolar cleft of HDM2, peptoids 5–10 were designed and synthesized (Figure 7). In this series of molecules, peptoids 5–7 each have a single hydrophobic, cleft-binding side chain replaced with a methyl group, while peptoids 8 and 9 have the order of these side chains scrambled, and peptoid 10 has a chlorine-substituted indole side chain. For the first set, replacing the hydrophobic side chain

with a methyl group decreased the binding affinity to HDM2, supporting the structural model. As compared to peptoid 4 (IC_{50} of 17.8 μM), the most significant loss in binding affinity was seen when the mimic of the phenylalanine side chain was replaced with a methyl group (peptoid 5, IC_{50} of 59.8 μM). This effect was less pronounced when side chains mimicking the tryptophan and leucine were replaced with methyl groups (peptoids 6 and 7, IC_{50} values of 28.3 and 25.3 μM , respectively). This is in contrast to the work of Böttger and co-workers,⁷ who found the tryptophan side chain to have the most stabilizing effect. In the second set of peptides, scrambling the positions of the hydrophobic side chains in the peptoid sequence (peptoids 8 and 9) lowered the binding affinity to a similar degree, as seen in peptoids 6 and 7. Finally, peptoid 10 was synthesized by analogy to the work of García-Echeverría and co-workers, who obtained significant improvement in binding affinity by substituting chlorine at the 6 position of the tryptophan indole moiety.^{5,20} They hypothesize that the chlorine increases the intermolecular van der Waals contact by filling a proximal cavity below the indole ring at the bottom of the HDM2 binding cleft. Similarly, peptoid 10 showed a significant decrease in the IC_{50} value from 17.8 to 9.9 μM (Figure 11A and Table 1). It should be noted, however, that the effect of the chloro-substitution was much larger for the peptides, with approximately 2 orders of magnitude reduction in the IC_{50} value.²⁰ Nevertheless, these results are consistent with the arrangement (i.e., p53 wild-type arrangement) of hydrophobic residues predicted to be energetically preferred for binding.

6. Residue Chirality. Although the CD spectrum of peptoid 4 suggests the absence of a helix in solution, the remaining four chiral residues in the sequence may still provide a conformational bias to the final, docked peptoid structure. To investigate the potential effects, peptoid 11 was synthesized with the

Table 2. K_d from Isothermal Titration Calorimetry

entry	K_d (μM) ^a
peptoid	
10	1.75 ± 0.22
13	1.23 ± 0.31
p53(15–29) peptide	0.62 ± 0.12

^a Titrations were performed in 10 mM Tris HCl, 150 mM NaCl, 1 mM β -mercaptoethanol, 0.5 mM EDTA, pH 7.6. All data were fit to a single site binding curve with 1:1 stoichiometry, from which K_d was calculated.

stereochemistry reversed for the first and third chiral *p*-nitrophenylethyl side chains (i.e., at positions 1 and 6), and peptoid 12 was synthesized with all achiral analogues (Figure 8). In fact, none of these modifications had a significant effect on the binding affinity to HDM2 (Figure 11A and Table 1). In addition, the aqueous solubility of peptoid 12 in buffer was the same (1.8 mM) as its chiral predecessor (peptoid 4). To investigate further, peptoid 13 was synthesized as an achiral version of peptoid 10. In this case, with the 6-chlorotryptophan substitution present, removal of the chirality resulted in a relatively small increase in the binding affinity, that is, a reduction in IC_{50} from 9.9 to 6.6 μM (Figure 11A and Table 1). Thus, the best peptoid inhibitor we obtained to this point lacked any of the originally designed stereocenters and contained the 6-chloro substitution on the tryptophan peptoid side chain. To eliminate any concerns that peptoid 13 could be aggregating into dimers, trimers, or tetramers, analytical ultracentrifugation of this peptoid strongly indicated that it is present as a monomer under the aqueous conditions used to test the binding (see the Appendix in the Supporting Information for details).

7. Role of One Central *p*-Nitro Group. To assess whether the central *p*-nitrophenylethyl groups play a role in binding to HDM2, one of these groups was changed to a hydroxy ethyl side chain, as seen in peptoid 14 (Figure 9). The binding of this peptoid to HDM2 was 2-fold weaker than that of peptoid 13, indicating that this side chain does contribute to binding.

8. Comparison with Other Molecules and Isothermal Titration Calorimetry (ITC). Additional experiments were performed to directly compare the affinities of peptoids 10 and 13 to those of three other HDM2-binding molecules in the literature, that is, the *a* and *b* enantiomers of Nutlin-3¹⁸ and the best HDM2-binder found from screening a large library of peptoids (Figure 10).⁹ We will refer here to the latter as the “Alluri peptoid”. Under the same conditions, Nutlin-3a and -3b bound HDM2 with IC_{50} values of 1.2 and 17.7 μM , respectively, as compared to 3.0 μM for the control p53 peptide (Table 1). Interestingly, while the IC_{50} value we obtained for the *b* enantiomer of Nutlin-3 was close to that previously reported by Vassilev and co-workers (i.e., 13.6 μM), they obtained a value approximately 1 order of magnitude smaller for the *a* enantiomer (i.e., 0.09 μM).¹⁸ In contrast, we did not detect any competitive binding for the Alluri peptoid using the fluorescent assay. Thus, the Alluri peptoid likely binds to the N-terminus of the HDM2 fragment at an alternate location than the p53 binding cleft. To further confirm the binding association of peptoids 10 and 13 to HDM2, isothermal titration calorimetry was performed to obtain dissociation constants (K_d) for the peptoids and the p53 peptide. As shown in Table 2 (and Figure 11B), the relative differences in K_d values are similar to the IC_{50} data obtained from fluorescence polarization.

Discussion

These results demonstrate that we have successfully developed an all-peptoid decamer that competes with the wild-type, N-terminal p53 peptide for the binding site of the N-terminal domain fragment of HDM2. Although not currently better than the p53 peptide, the IC_{50} and dissociation constant for peptoid 13 are only approximately 2-fold larger (Figure 11, Tables 1 and 2). Our structure-based design approach, which involved iterative cycles of computer model building, led us to the initial peptoids that showed only weak binding to HDM2. Three synthetic modifications to the side chains of the initial peptoids allowed significant improvement in the binding affinity. The first major improvement came by introducing three phosphonate-containing side chains at positions 4, 7, and 9 to increase the aqueous solubility and, according to modeling, potentially form salt-bridges with positively charged residues around the HDM2 binding cleft (Figure 4). Subsequent substitutions with neutral sulfonamides showed that the third phosphonate group does not significantly affect binding (peptoid 4). The next major improvement came with the addition of *para*-nitro substitutions on the phenyl rings of the four (*S*)-*N*-(1-phenylethyl)glycine side chains at positions 1, 3, 6, and 10 (peptoid 3). As described in the Results, the enhanced affinity may be due to a number of factors, including favorable interactions with proximal residues of HDM2. Support for this comes from the finding that deletion of both the N- and C-terminal (*S*)-*N*-(*p*-nitrophenylethyl)glycine residues drastically reduces the binding affinity, and in the modeled complex these nitro groups could interact with the positively charged K94 and R97 residues of HDM2. Furthermore, replacement of the *p*-nitrophenyl group at position 3 with a hydroxyethyl group (peptoid 14) also decreased the HDM2 binding affinity, indicating that this central *p*-nitrophenyl group interacts favorably with HDM2. The final improvement came with the substitution of chlorine at the 6 position of the indole ring of the tryptophan peptoid analogue (peptoids 10 and 13). A similar result, although of greater magnitude, was found in the development of peptide-based inhibitors of the same HDM2 target.²⁰

The reduced binding affinities of peptoids 5–9 as compared to peptoid 4 (Table 1) indicate that the peptoid side chains that mimic the phenylalanine, tryptophan, and leucine of the p53 peptide each play roles in stabilizing the complex, similar to the p53 peptide. Furthermore, the improvement in binding affinity seen with the introduction of the 6-chloroindole side chain (peptoid 10) has some correlation with the improvement in binding seen with HDM2-binding peptides containing 6-chlorotryptophan. The structural explanation provided by García-Echeverría and co-workers is that the chlorine fills a cavity in the binding cleft below the indole moiety.²⁰ While it is tempting to assume that the three hydrophobic peptoid residues all bind in the nonpolar cleft of HDM2, consistent with early peptide studies,⁷ the crystal structure,³ and our computer generated model, this may not be the case. For all of these control peptoids (peptoids 5–10), the changes in binding affinity are significantly less dramatic than the corresponding changes observed in HDM2-binding peptides. Furthermore, the requirement for nitro groups to be present on several of the peptoid side chains indicates that there are important peptoid–HDM2 interactions that do not involve the hydrophobic side chains.

Another major question concerns the conformation of the

peptoid backbone when bound to HDM2. Although initially designed with chiral (*S*)-*N*-(1-phenylethyl)glycines to have a right-handed type-I polyproline helical conformation, our optimizations led to peptoid 13, which is devoid of chiral side chains. Because of the synthetic difficulty, it is not feasible at the present time to make a derivative of peptoid 13 in which each side chain contains a helix-promoting stereogenic carbon at every position. Because the steric bias provided by each (*S*)-*N*-(1-phenylethyl)glycine has been calculated to be as small as 0.5 kcal/mol between right- and left-handed helical conformations in solution,¹³ it is understandable that mixing chiral and achiral groups results in peptoids that are not fully helical in solution, as indicated by the CD data. While it is possible that a helical conformation in the peptoid may be induced by binding to HDM2, alternate peptoid conformations could also be induced by the energetics of binding. Indeed, through modeling we were able to identify other, nonhelical conformations of the peptoid backbone that could be relevant to binding HDM2 (results not shown). Therefore, the helical peptoid conformation shown in Figure 4 may not be very accurate, but it does demonstrate that stabilizing, intermolecular interactions can form between the peptoid's two phosphonate-containing residues, the N- and C-terminal nitrophenyl groups, and, by analogy, the sulfonamide group. This model also places the hydrophobic side chains into the binding cleft of HDM2. We are currently attempting to determine the crystal structure of this complex to answer these questions and provide a more confident basis to design further optimizations. In addition, it will show if the peptoid binding induces a conformation in the HDM2 fragment different from that in the original crystal structure with the wild-type p53 peptide.²⁴

(24) Schon, O.; Friedler, A.; Freund, S.; Fersht, A. R. *J. Mol. Biol.* **2004**, *336*, 197–202.

Our study has identified many important details about using a peptoid oligomer to mimic a specific bioactive peptide. In contrast to our initial predictions, the achiral peptoids were the best HDM2 binders rather than the peptoids with helical structures. Such results indicate that peptoids can adopt conformations that are nonhelical, which are important for binding to proteins. While the results we present in this paper do not compete with many recently published studies of HDM2 inhibition with regard to drug development,^{5,10,20} they do reveal a number of important elements to consider when using peptoids to inhibit protein–protein interactions. Our future structural studies will likely guide our development of additional peptoid side chains that can further enhance binding to HDM2 as well as identify new ways to design peptoids to inhibit other protein–protein interactions.

Acknowledgment. This research was supported in part by the following Intramural Research Programs of the NIH: NCI Center for Cancer Research and NIDDK Laboratory of Bioorganic Chemistry. M.C.M. was supported by a graduate student fellowship from Abbott Laboratories while at Northwestern University. We are grateful to Dr. Vassilev at Hoffman LaRoche for providing a sample of the Nutlins. We would also like to thank Dr. Marc S. Lewis for performing the analytical ultracentrifugation experiments.

Supporting Information Available: Synthetic procedures and characterization for all new peptoid monomers and peptoid oligomers. Experimental procedures for circular dichroism, fluorescence polarization, and isothermal titration calorimetry. Complete author lists for refs 10h, 10j, 12a, 12c, 12d, 17, 18, 19b, and 23. This material is available free of charge via the Internet at <http://pubs.acs.org>.

JA056344C